Stochastic Analysis of Nusselt Numbers for Natural Convection with Uncertain Boundary Conditions

Bettina Schieche* and Jens Lang, March 24, 2010
*schieche@gsc.tu-darmstadt.de

TECHNISCHE UNIVERSITÄT DARMSTADT

GRADUATE SCHOOL computational engineering

Center of Smart Interfaces

Abstract

In this report, an example for natural convection in a 2-dimensional system is considered, described by the thermally coupled Navier-Stokes equations. The boundary conditions are assumed to be uncertain and are modelled by correlated stochastic processes. In order to solve such a Partial Differential Equation (PDE) with uncertain input, we apply a Stochastic Collocation method, which basically discretizes the underlying sample space in a geometric way. The quantity of interest is the heat exchange at the surface of the system, measured by Nusselt numbers. The main goal of this work is the stochastic analysis of these Nusselt numbers by comparing the input fluctuation with the standard deviation of the response.

1 Introduction of the Problem

Thermally coupled flow can be modelled by the Navier-Stokes equations coupled with the heat equation using the Boussinesq approximation. The setting focused in this work is taken from [8]. We consider a system of two spatial dimensions, which is illustrated in Fig. 1. No-slip boundary conditions are applied,

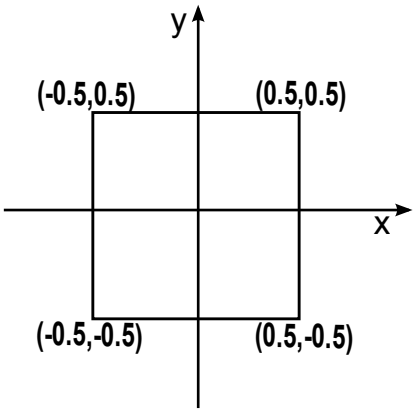

Figure 1: Illustration of the computational domain.

i.e. vanishing velocity at all four walls. The corresponding dimensionless equations are given by

$$\begin{aligned} \frac{\partial u}{\partial t} + (u \cdot \nabla)u - 2Pr \cdot \operatorname{div}(\epsilon(u)) + \nabla p &= -Pr\, Ra\, T\, g \\ \operatorname{div}(u) &= 0 \\ \frac{\partial T}{\partial t} + (u \cdot \nabla)T - \Delta T &= 0, \end{aligned} \tag{1}$$

with velocity u, temperature T and pressure p (see e.g. [5]). The vector g describes the normalized gravity in the system and $\epsilon = 0.5(\nabla u + \nabla u^T)$ denotes the strain tensor. The dimensionless values Pr and Ra are the Prandtl and Rayleigh number and are set to 1 and 5000, respectively. At the left wall a constant temperature of $T(-0.5, y, t) = 0.5$ is applied, whereas the temperature at the right wall is assumed to be not explicitly known. This uncertainty is described by the time-independent stochastic boundary condition $T(0.5, y, t) = \alpha(y, \omega)$ with mean -0.5 and standard deviation σ. The variable ω is random and is thus chosen from a sample space Ω. The lower and upper walls are assumed to be thermally insulated, i.e. we set $n \cdot \nabla T = 0$ there.

2 Simplification of the Stochastic Boundary Condition

The uncertain temperature at the right boundary is modelled by the random process $\alpha(y, \omega)$ as already mentioned in section 1. This process is assumed to be Gaussian, meaning that it equals a normal dis-

tributed random variable for every fixed $y \in [-0.5, 0.5]$. An important part of modelling consists in the assumption that the random variable corresponding to any point y_1 is correlated with any other point y_2. Hence, the randomness is not modelled by white noise, but by an autocorrelated random process with a covariance function $C_\alpha(y_1, y_2)$. Such a problem is called PDE with random coefficients. Here, the correlation function is given by

$$C_\alpha(y_1, y_2) = \sigma^2 \exp\left(-\frac{|y_1 - y_2|}{c}\right) \tag{2}$$

with correlation length $c = 1$. The correlation length is a measure for the distance between two points in space which are still strongly correlated. The normalized function $C_\alpha(y_1, y_2)$ is shown in Fig. 2. It can be seen that the covariance decreases the larger the distance between two points at the considered wall becomes. In order to deal with the stochastic boundary condition, the random process $\alpha(y, \omega)$ has

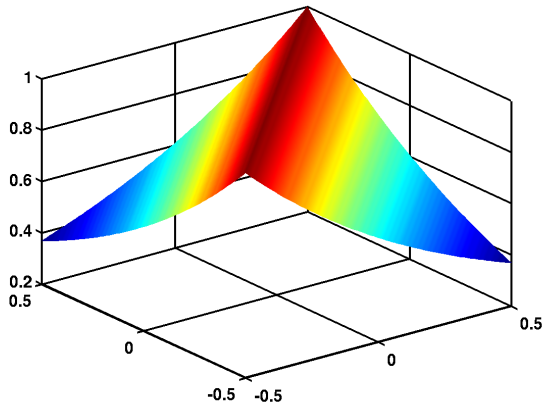

Figure 2: Correlation function for the right (uncertain) boundary condition.

to be separated in a deterministic and a stochastic part. This is done by the so-called Karhunen-Loève expansion ([2],[3]), resulting in the following infinite sum

$$\alpha(y, \omega) = -0.5 + \sum_{n=1}^{\infty} \xi_n(\omega) \sqrt{\lambda_n} f_n(y) \tag{3}$$

with uncorrelated standard normal distributed random variables $\{\xi_n\}_{n\in\mathbb{N}}$ and deterministic functions $\{f_n(y)\}_{n\in\mathbb{N}}$. These functions together with the constants $\{\lambda_n\}_{n\in\mathbb{N}}$ are solutions of the integral-eigenvalue problem

$$\int_{-0.5}^{0.5} C_\alpha(y_1, y_2) f_n(y_2)\, \mathrm{d}y_1 = \lambda_n f_n(y_2), \tag{4}$$

which can be solved analytically by differentiating the whole integral equation twice with respect to y_1 and then solving the resulting ordinary differential equation.

The eigenvalues tend to zero with growing n and hence, the next step of proceeding is to truncate the infinite expression for α in (3) after N terms:

$$\alpha(y, \omega) \approx \alpha(y, \xi_1, \xi_2, ..., \xi_N) := -0.5 + \sum_{n=1}^{N} \xi_n \sqrt{\lambda_n} f_n(y). \tag{5}$$

In our example, N can be chosen very small since the eigenvalues decrease rapidly and thus the truncation error becomes already small. Approximation (5) is now taken as the temperature boundary condition for small N.

3 Stochastic Collocation

Since there is an uncertainty in the input parameters of PDE (1), the velocity, temperature and pressure are of course also random processes depending on the same random variables $\{\xi_n\}_{n=1}^N$ describing the input uncertainty. Solutions are assumed to have finite variance for every point in space, such that an appropriate stochastic solution space is the space of all square-integrable random variables equipped with the N-dimensional Gaussian probability measure. This space is denoted by $L^2(\Omega)$.

The randomness is handled as an extra dimension in addition to space and time. For numerical treatment it has to be discretized. For that, not the sample space Ω itself is taken, but the corresponding image space under the considered probability measure. Uncorrelated normal distributed random variables are stochastically independent and so, the image space is equal to $\mathbb{R}^N$, which is now going to be discretized.

A set of M nodes $\{z_k\}_{k=1}^M$ is chosen within $\mathbb{R}^N$, where each node represents a certain image of the N-tuple $(\xi_1, ..., \xi_N)$. These numbers are put into expression (5), resulting in a deterministic boundary condition for each node. So, PDE (1) has to be solved with M different deterministic boundary conditions, which can be done separately. The resulting solutions are then interpolated by Lagrange polynomials in order to get a continuous representation. The challenge is the placement of the nodes, which is explained in section 7. As an example, the solution process for the temperature in the system can now be expressed by

$$T(x, y, t, z) \approx \sum_{k=1}^{M} T_k(x, y, t) L_k(z) \tag{6}$$

with T_k being the deterministic temperature solution for collocation point z_k. The functions L_k represent certain tensor products of Lagrange polynomials ([7]). Note, that as for classical Lagrange interpolation it holds

$$L_k(z_l) = \begin{cases} 1 \text{ if } k = l \\ 0 \text{ if } k \neq l. \end{cases} \tag{7}$$

The whole procedure is called Stochastic Collocation and the nodes $\{z_k\}_{k=1}^M$ are called collocation points. A detailed description of the method is given in [13],[12] or [1], for example. A more mathematical point of view is presented in [4] or [11]. It is clear that the method also allows solution expressions for the velocity components and the pressure.

4 Solving the Deterministic PDE

Stochastic Collocation requires solving the deterministic Boussinesq equation in each collocation point, namely M times for different boundary conditions. Here, this is done by the state-of-the-art PDE-solver KARDOS. Stabilized linear finite elements ([9]) are used, which are known to work well for the given problem.

Time runs from $t_0 = 0$ until a steady state is reached, which is approximately the case at time $t_1 = 6$. Integration is performed adaptively using a Rosenbrock type method of order 3. The initial temperature profile must be consistent with the boundary conditions to avoid discontinuities. One could just interpolate the temperature condition of the two vertical walls linearly, but physically it makes more sense to take an exponential profile since this might reflect a sudden heating or cooling in a better way. Such an initial profile for the mean temperature -0.5 for example can be seen on the left picture of Fig. 3. Nevertheless, a sudden heating respectively cooling of the system is difficult to simulate, meaning that the algorithms need some time to find a state that makes sense from a physical point of view. In order to let KARDOS find such a state, the first 5 time steps are done with constant step size of 10^{-3} and after that the adaptive step size control is switched on.

In space a fixed grid of 4225 is chosen, which can be seen on the right picture of Fig. 3. The given problem is constructed such that the fluid will perform some kind of circular movement. The velocity is forced to zero at the boundary, and so the steepest changing of the velocity field is expected to take place near the boundary. This knowledge gives rise to construct a grid which is finer in the boundary regions than in the middle and point symmetric about the center of the system.

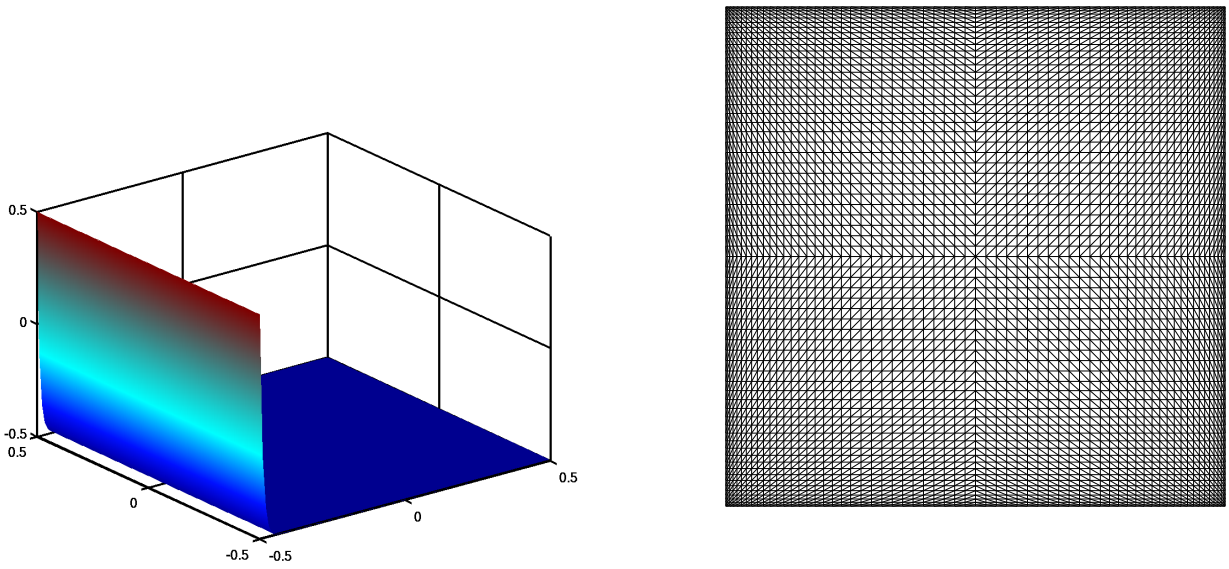

Figure 3: Left: initial temperature profile, right: spatial triangulation.

5 Quantitiy of Interest: Nusselt Numbers

An important quantity of interest for the considered problem is the Nusselt number ([10], [6]). It is a measure for the heat exchange at surfaces and thus a common efficiency measure. Here, the Nusselt numbers for the steady state at both the left and right wall is of interest. Mathematically, the stationary Nusselt numbers $\mathrm{Nu}_{\mathrm{left}}$ and $\mathrm{Nu}_{\mathrm{right}}$ for the left and right wall are defined by

$$\mathrm{Nu}_{\mathrm{left}} = \frac{1}{A}\int_{-0.5}^{0.5} -\frac{\partial T}{\partial x}|_{x=-0.5}\,\mathrm{d}y \text{ and} \tag{8}$$

$$\mathrm{Nu}_{\mathrm{right}} = \frac{1}{A}\int_{-0.5}^{0.5} -\frac{\partial T}{\partial x}|_{x=0.5}\,\mathrm{d}y. \tag{9}$$

The constant A is a scaling factor and can be chosen in different ways. For natural convection an appropriate choice is the temperature difference between both vertical walls, which is just equal to 1 in our case. Note that Nusselt numbers have to be approximated by quadrature rules, which is simply realized by the composed midpoint rule.

6 Statistics of the Solution

Since the collocation solution alone does not provide a real understanding of the considered system, one has to look at certain statistical quantities like the first moments of the velocity, temperature and Nusselt

numbers. Stochastic postprocessing requires solving integrals weighted by the density function $\rho(z)$. This density function is here given by

$$\rho(z) = \frac{1}{(2\pi)^{N/2}} \exp\left(-\frac{1}{2}\|z\|_2^2\right). \tag{10}$$

Exemplarily, calculating statistics is illustrated for the Nusselt number of the left wall. It can be written as (compare equation (6))

$$\mathrm{Nu}_{\mathrm{left}}(z) \approx \sum_{k=1}^{N} (\mathrm{Nu}_{\mathrm{left}})^{(k)} L_k(z), \tag{11}$$

where $(\mathrm{Nu}_{\mathrm{left}})^{(k)}$ is the Nusselt number obtained by solving the deterministic problem for collocation point z_k. Its corresponding expected value can thus be calculated as follows:

$$\mathrm{E}[\mathrm{Nu}_{\mathrm{left}}(z)] = \int_{[-\infty,\infty]^N} \mathrm{Nu}_{\mathrm{left}}(z)\rho(z)\,\mathrm{d}z = \sum_{k=1}^{M} \mathrm{Nu}_{\mathrm{left}}^{(k)} \int_{[-\infty,\infty]^N} L_k(z)\rho(z)\,\mathrm{d}z. \tag{12}$$

There arises one integral for each collocation point, which can hardly be solved analytically. Hence, one needs to proceed via quadrature rules. For that, it is important to take the density function into account and construct rules for weighted integrals. A natural decision for quadrature nodes would be the collocation points themselves. Actually this linkage is used the other way around. One chooses the collocation points $\{z_k\}_{k=1}^M$ with respect to adequate quadrature rules for the stochastic postprocessing. Such a quadrature rule with weights $\{w_k\}_{k=1}^M$ and the use of equation (7) provide the simple formula

$$\mathrm{E}[\mathrm{Nu}_{\mathrm{left}}(z)] \approx \sum_{k=1}^{N} w_k \mathrm{Nu}_{\mathrm{left}}^{(k)}. \tag{13}$$

For the second moment the procedure is exactly the same. The formula differs only in the square of the solution:

$$\mathrm{E}[\mathrm{Nu}_{\mathrm{left}}^2(z)] \approx \sum_{k=1}^{M} w_k (\mathrm{Nu}_{\mathrm{left}}^{(k)})^2. \tag{14}$$

This way, any statistical quantity can easily be obtained.

7 Choice of Collocation Points

The close connection between collocation points and quadrature rules has already been explained in section 6. Since the dimension of any statistical integral (see e.g. (12)) is determined by the number of considered random variables, the main task is to find grids on high dimensional cubes. A brute force quadrature technique for high dimensional cubes is to consider a 1-dimensional quadrature rule and take its tensor product for a multidimensional version. The problem with that is the very large number of resulting collocation points even for only a few dimensions. Hence, the goal is to construct efficient sparse grids ([15]). The commonly used method for the construction of sparse grids is the Smolyak algorithm.

Smolyak Algorithm

Smolyak's algorithm ([20]) also starts with quadrature rules in one dimension, namely a sequence of such rules $\{U^i\}_{i=0,1,2,...}$

$$\int f(z)\,\mathrm{d}z \approx U^i(f) = \sum_{j=1}^{m_i} f(z_j^i)\cdot w_j^i \tag{15}$$

with given natural numbers m_i. Let now $\Delta^0 := U^0$, $\Delta^i := U^i - U^{i-1}$, $i > 0$, denote the corresponding difference formulas. Then Smolyak's algorithm is given by

$$A(k,d) = \sum_{\|\mathbf{i}\|_1 \le d+k} (\Delta^{i_1} \otimes \cdots \otimes \Delta^{i_d}). \tag{16}$$

The number k in this expression is a natural number and is called Smolyak level, whereas $\mathbf{i} := (i_1, ..., i_d)$ denotes an index, whose components refer to the rules in equation (15). This rule combines quadrature rules of different cardinality in all dimensions. So, one can use formulas with high degree of exactness without getting a full grid.

The main idea in using Smolyak's algorithm consists in chosing the 1-dimensional quadrature rules in equation (15) such that they are nested. This means that each set of nodes is a subset of the next bigger set. Usually one starts with a rule of only one point and then adding points successivley. Then the nested character of the nodes is known to be transferred to the multidimensional Smolyak rule $A(q,d)$ ([20],[19]). So, increasing the Smolyak level k does not change the whole grid, but only adds new points to already existing nodes. In this case, the difference formulas Δ^i can be seen as an update of a coarser rule.

Nested rules also provide the possibility of efficient error estimation, namely a rule is assumed to be good enough if refinement of the grid does not contribute much to the integral approximation anymore.

Clenshaw-Curtis Nodes

In the context of Stochastic Collocation, usually Clenshaw-Curtis nodes ([16]) are used. The rule is based on a Fourier expansion of the integrand and the resulting nodes equal the extremums of Chebyshev polynomials. The advantage of Clenshaw-Curtis rules is that they can easily be nested and in addition reduce oscillation effects in the boundary regions. That is why they are often preferred to Newton-Cotes-formulas.

Fig. 4 shows example grids in two dimensions referring to two random variables to describe the uncertainty. The grids are constructed by Smolyak's algorithm using nested Clenshaw-Curtis rules. Step by step the Smolyak level is increased, where the newly added nodes are marked in red. The sparse structure of the grid is obvious.

Smolyak's algorithm given by equation (16) is characterized by the dimension of the integral to be solved and the Smolyak level. The admissible terms in the sum are given by the criterion $\|i\|_1 <= d + k$. It is possible to use other admissible sets of indices. One example is the so-called generalized Smolyak algorithm ([17],[18]), often also denoted as anisotropic version since it adaptively adds more nodes in dominant directions of the space.

Here, a balanced version of both isotropic and anisotropic Smolyak algorithm has been used in order to take the decreasing importance of random variables into account. The first random variable arising in the Karhunen-Loève-expansion (see equation (5)) is clearly the dominant direction and contributes most to any statistical quantity of the solution. Since the Nusselt numbers at the vertical walls are seen to provide the key information for the problem, their standard deviation is used for error estimation. Nodes are successively added in the direction of most contribution to the standard deviation of the Nusselt number. This is done until the relative contribution falls under a tolerance of 10^{-3}.

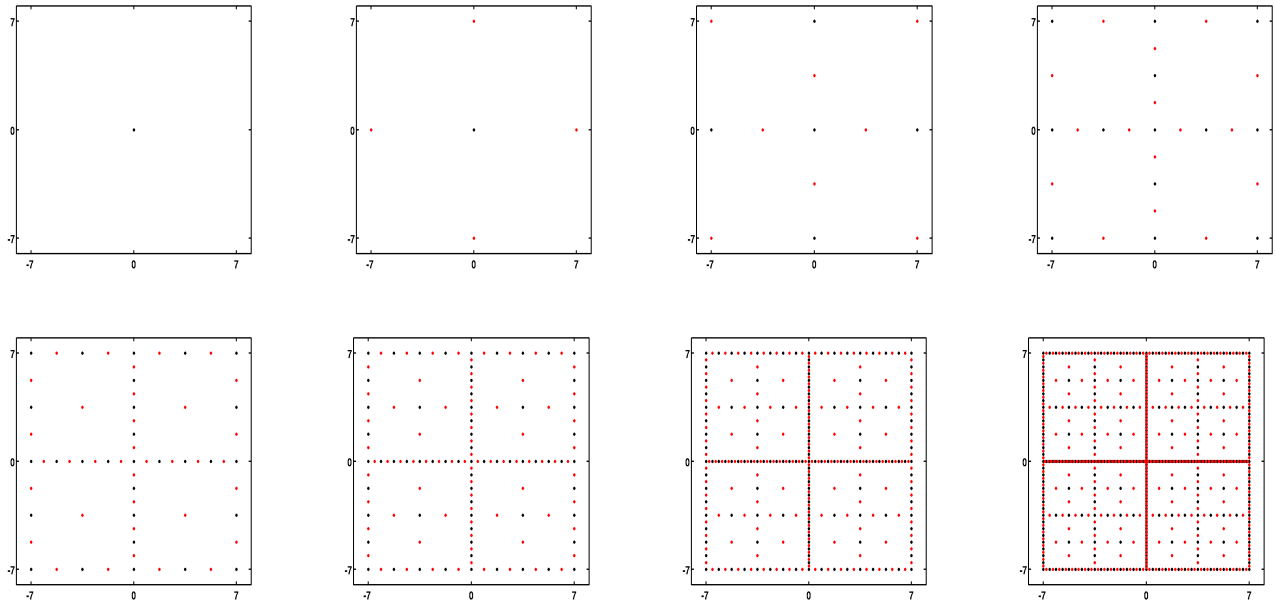

Figure 4: Smolyak grid in 2 dimensions up to level 7, constructed by Clenshaw-Curtis nodes.

8 Results

All results are presented for the steady state of the system. They are not compared to [8], because the paper does not consider the Nusselt number and in addition is using slightly other solving procedures.

The whole problem was solved for 2, 4 and 6 random variables and an input standard deviation σ of 0.2, 0.4 and 0.6. Fig. 5 shows the vector field of the expected value (left) and standard deviation (right) of the resulting velocity for $N = 6$ and $\sigma = 0.2$. One can see that the fluid starts moving in a circle as expected due to gravity and the temperature difference. For the standard deviation the vectors of course point in positive direction. The faster the mean velocity the bigger is also its standard deviation. This makes sense since a bigger activity of the fluid gives rise to larger fluctuation.

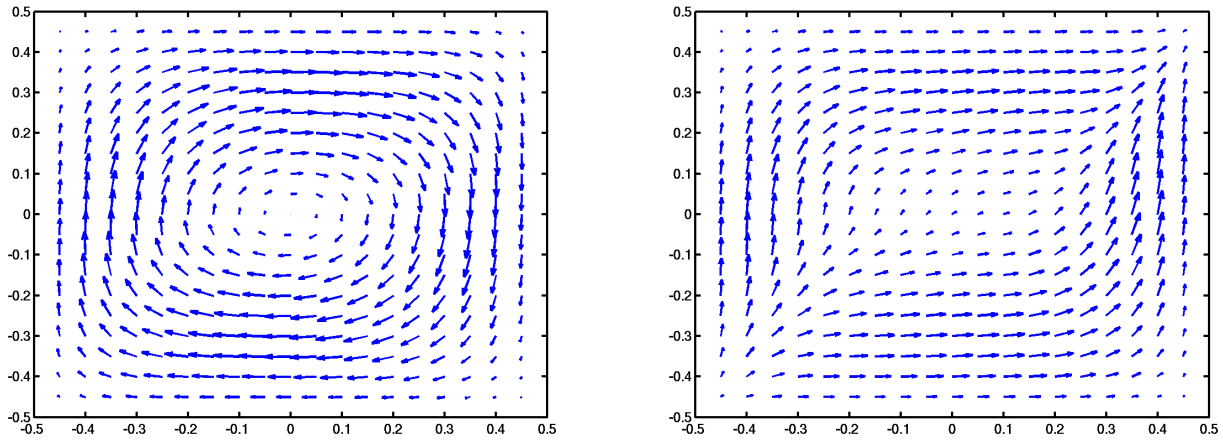

Figure 5: Expectation and standard deviation of steady state velocity.

Fig. 6 shows the result for the steady state expectation of the temperature as surface and contour plot. One can not only recognize the deterministic boundary condition on the left wall, but also the expectation of the stochastic boundary condition on the right wall, which is exactly resolved. Truncating the Karhunen-Loève expansion does not influence the expectation of the random process α. In addition the quadrature rules are constructed such that constant values with respect to the density ρ are integrated exactly. So, both steps do not give rise to error sources for the expectation on the right wall.

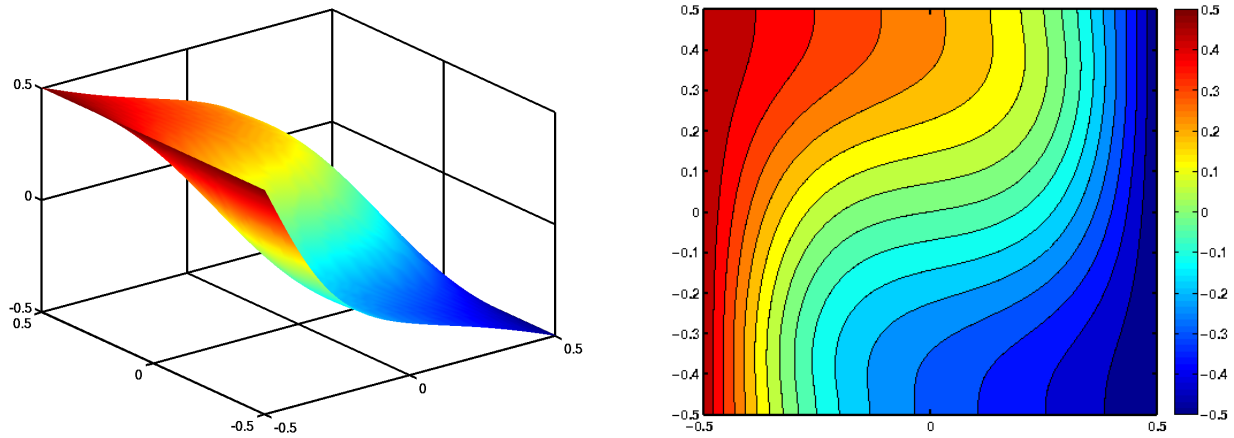

Figure 6: Expectation of steady state temperature.

In Fig. 7 the standard deviation of the steady state temperature for different input standard deviations is shown. The left picture corresponds to $\sigma = 0.2$, the middle one to $\sigma = 0.4$ and the right one to $\sigma = 0.6$. All three pictures have been obtained using 6 random variables which results in a 6-dimensional stochastic space. Here, quadrature rules do not distort the solution either, but truncation of the Karhunen-Loève-expansion results in an error. One can observe that the input standard deviation is resolved quite well, but of course not exactly.

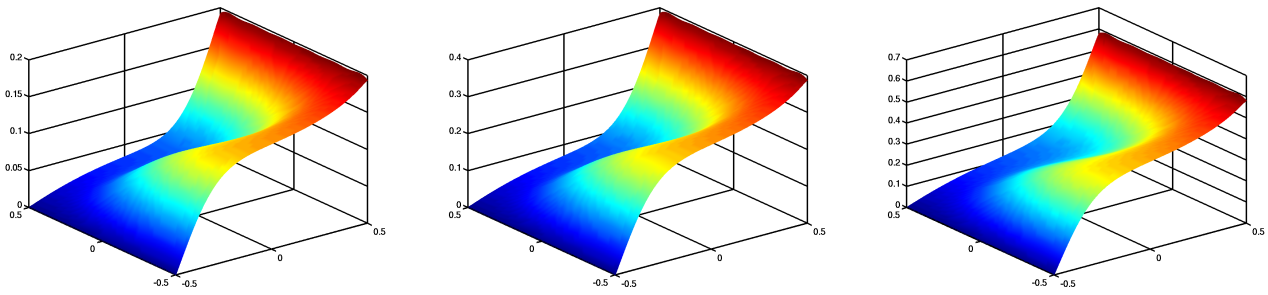

Figure 7: Standard deviation of steady state temperature, $\sigma = 0.2$, $\sigma = 0.4$, $\sigma = 0.6$.

The solutions for $N = 2$ and $N = 4$ are not shown, because the corresponding pictures all look pretty much like the ones shown here. Since the quantity of interest is the Nusselt number, this number was actually taken to compare all the solutions. Tab. 1 shows the resulting expectation and standard deviation of the Nusselt numbers for both walls. One can see that the steady state of the system results in similar Nusselt numbers on both walls which is not surprising since the problem is completely symmetric - at least for the mean of the input uncertainty. Another important observation is that the number of random variables do not influence the Nusselt number significantly. In most of the cases the first two to

three decimal places agree. So, one does not have to use highdimensional stochastic spaces and thus get along with less collocation points.

An interesting phenomenon can also be derived from the Nusselt numbers in Tab. 1. The standard deviation seems to be the result of a multiplication of the input standard deviation with a factor very close to 2. For $\sigma = 0.2$ the output Nusselt numbers are close to 0.4, for $\sigma = 0.4$ the output Nusselt numbers are close to 0.8 and for $\sigma = 0.6$ the output Nusselt numbers are close to 1.2. This observation shows that the variance of the Nusselt number continuously depends on the input fluctuation in this example. This dependence is important, because it means that no unpredictable behaviour in the system happens due to distorted boundary conditions. It would be worth analysing this effect in a more general and analytical manner.

Expectation left wall	$\sigma = 0.2$	$\sigma = 0.4$	$\sigma = 0.6$
2 random variables	1.80908	1.85123	1.92289
4 random variables	1.80917	1.85160	1.92438
6 random variables	1.80918	1.85162	1.92382
Expectation right wall	$\sigma = 0.2$	$\sigma = 0.4$	$\sigma = 0.6$
2 random variables	1.80871	1.84978	1.91990
4 random variables	1.80884	1.85029	1.92158
6 random variables	1.80884	1.85032	1.92109
Standard deviation left wall	$\sigma = 0.2$	$\sigma = 0.4$	$\sigma = 0.6$
2 random variables	0.41917	0.82826	1.22672
4 random variables	0.41939	0.82858	1.22680
6 random variables	0.41939	0.82860	1.22636
Standard deviation right wall	$\sigma = 0.2$	$\sigma = 0.4$	$\sigma = 0.6$
2 random variables	0.42364	0.83695	1.23900
4 random variables	0.42452	0.83871	1.24142
6 random variables	0.42456	0.83879	1.24086

Table 1: Expectation and standard deviation of steady state Nusselt numbers.

Tab. 2 shows the nodes for all considered combinations of σ and N, that were necessary to reach the above mentioned tolerance of 10^{-3} for Smoylak's algorithm. It can be seen that the number of required nodes increases both with the number of random variables and the input standard deviation σ. The first effect is clear since a higher dimension requires more nodes to capture the whole space. The second effect is also not surprising. A larger fluctuation in the system naturally requires more information to resolve the dynamics adequately and this is reflected by the need for more collocation points.

	$\sigma = 0.2$	$\sigma = 0.4$	$\sigma = 0.6$
2 random variables	69	109	165
4 random variables	117	145	197
6 random variables	121	181	285

Table 2: Number of needed nodes.

Fig. 8 shows the resulting collocation points within the stochastic space for $\sigma = 0.6$ and $N = 6$. In all five pictures the nodes corresponding to the first random variable are plotted in x-direction. In y-direction the nodes correspond to the 2nd till 5th random variable (from left to right). As predicted in section 7,

the first random variable appears to be the dominant dimension, wheras all the other directions decrease in their importance.

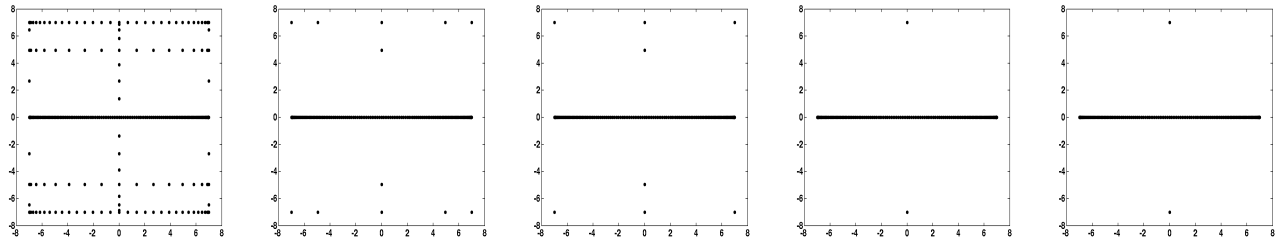

Figure 8: Smolyak grids: 1st random variable plotted against 2nd-6th random variable.

9 Summary and Conclusion

Natural convection with stochastic boundary conditions in a 2-dimensional system has been simulated. Such a problem can be solved using Stochastic Collocation resulting in as many deterministic problems as collocation points. The position of collocation points is closely related to quadrature rules, which are chosen with respect to the probability measure of the stochastic boundary condition. The problem has been solved for different input standard deviations using stochastic spaces up to dimension 6. The quantity of interest for all test cases was the Nusselt number at the vertical walls of the system in order to measure the heat exchange. The main result is that the standard deviations of the resulting Nusselt numbers depend on the input fluctuation by a factor very close to 2 in the given problem, which means that the stochastic condition does not distort the system in an uncontrollable way.

Stochastic Collocation is similar to Monte Carlo simulation in terms of the calculation procedure. In both techniques a number of nodes is chosen and put into the PDE seperately. The resulting deterministic problems can be solved independently and with respect to computational effort in parallel. The difference lies in the choice of the stochastic nodes. Stochastic Collocation uses sort of geometric grids, whereas Monte Carlo choses the nodes randomly according to the given probability measure. Calculation of statistical quantities in both methods basically mean evaluation of sums. The big hope of Stochastic Collocation is the immense reduction of nodes by using not only sparse grids, but also adaptive procedures. Monte Carlo simulation often lacks in stable solutions unless the random numbers are increased up to an exorbitant number. The efficient use of Adaptive Stochastic Collocation depends on the dimension of the problem, but it seems to be a promising alternative to Monte Carlo simulations in many applications.

The idea of stochastic input data can be extended to many other applications and is not restricted to boundary conditions. Material properties, forcing terms or even the topology of the system can be treated as an uncertainty ([14]).

Acknowledgement

The authors gratefully acknowledge the support of the DFG Graduate School of Excellence Computational Engineering and the DFG Excellence Cluster Smart Interfaces - Understanding and Designing Fluid Boundaries.

10 References

[1] R. C. Almeida. Stochastic finite element techniques for transport equations. Technical report, The Institute for Computational Engineering and Sciences, University of Texas at Austin, June 2009.

[2] R. B. Ash. *Real Analysis And Probability.*, pages 335–335. New York, Academic Press, 1972.

[3] R. B. Ash and M. F. Gardner. *Topics in Stochastic Processes.*, volume 27. New York: Academic Press, 1975.

[4] I. Babuška, F. Nobile, and R. Tempone. A stochastic collocation method for elliptic partial differential equations with random input data. *SIAM J. Numer. Anal.*, 45(3):1005–1034, 2007.

[5] R. Codina. *A Finite Element Formulation for Viscous Incompressible Flows.* Barcelona: CIMNE., 1993.

[6] G. Evans and S. Paolucci. The thermoconvective instability of plane poiseuille flow heated from below: A proposed benchmark solution for open boundary flows. *International Journal For Numerical Methods In Fluids*, 11:1001–1013, 1990.

[7] J. Foo, X. Wan, and G. E. Karniadakis. The multi-element probabilistic collocation method (me-pcm): Error analysis and applications. *J. Comput. Phys.*, 227(22):9572–9595, 2008.

[8] B. Ganapathysubramanian and N. Zabaras. Sparse grid collocation schemes for stochastic natural convection problems. *J. Comput. Phys.*, 225(1):652–685, 2007.

[9] J. Lang. Adaptive incompressible flow computations with linearly implicit time discretization and stabilized finite elements. *Computational Fluid Dynamics*, 1:200–204, 1998.

[10] X. Ma and N. Zabaras. An adaptive hierarchical sparse grid collocation algorithm for the solution of stochastic differential equations. *J. Comput. Phys.*, 228(8):3084–3113, 2009.

[11] F. Nobile, R. Tempone, and C. G. Webster. A sparse grid stochastic collocation method for partial differential equations with random input data. *SIAM J. Numer. Anal.*, 46(5):2309–2345, 2008.

[12] D. Xiu. Fast numerical methods for stochastic computations: A review. *Commun. Comput. Phys.*, 5(2-4):242–272, 2008.

[13] D. Xiu and J. S. Hesthaven. High-order collocation methods for differential equations with random inputs. *SIAM J. Sci. Comput.*, 27(3):1118–1139, 2005.

[14] D. Xiu and D. M. Tartakovsky. Numerical methods for differential equations in random domains. *SIAM J. Sci. Comput.*, 28(3):1167–1185, 2006.

[15] H. J. Bungartz and M. Griebel. Sparse grids. *Acta Numerica*, 13:147–269, 2004.

[16] C. W. Clenshaw and A. R. Curtis. A method for numerical integration on an automatic computer. *Numer. Math.*, 2:197–205, 1960.

[17] T. Gerstner and M. Griebel. Dimension-adaptive tensor-product quadrature. *Computing*, 71(1):65–87, 2003.

[18] W. A. Klimke. *Uncertainty Modeling Using Fuzzy Arithmetic and Sparse Grids.* Industriemathematik und Angewandte Mathematik. Aachen: Shaker Verlag; Stuttgart: Univ. Stuttgart, Institut für Angewandte Analysis und Numerische Simulation, 2006.

[19] E. Novak and K. Ritter. Simple cubature formulas with high polynomial exactness. *Constructive Approximation*, 15(4):499–522, 1999.

[20] E. Novak and K. Ritter. High dimensional integration of smooth functions over cubes. *Numer. Math.*, 75(1):79–97, 1996.